JOURNAL OF PHYSICAL ORGANIC CHEMISTRY
J. Phys. Org. Chem. 2004; **17:** 71–82
Published online 14 November 2003 in Wiley InterScience (www.interscience.wiley.com). DOI: 10.1002/poc.694

Influence of arene–arene interactions on the conformation of acyclic molecules: ^{1}H NMR and dipole moment experimental results

Pablo Bello,[1] Nicholas J. Heaton,[1†] Antonio Chana,[2] Jesús Jiménez-Barbero,[2] Evaristo Riande[1] and Bernardo Herradón[2]*

[1]Instituto de Ciencia y Tecnología de Polímeros, CSIC, Juan de la Cierva 3, 28006 Madrid, Spain
[2]Instituto de Química Orgánica, CSIC, Juan de la Cierva 3, 28006 Madrid, Spain

Received 19 February 2003; revised 3 June 2003; accepted 27 June 2003

ABSTRACT: Conformational analysis of derivatives of 2-methyl-1,3-propanediol is reported. The diol spacer is substituted with different aromatic residues that are linked by ether or ester functionalities. Most of the experimental evidence was obtained by ^{1}H NMR spectroscopy through the analysis of the vicinal coupling constants of the two ABX systems of the spacer. It is found that the main factor influencing the conformation of the molecules is the interaction between the aromatic fragments at the ends of the spacer. Thus, when the electronic character of the two residues is similar (e.g. **1**–**3** and **5**), the molecules have high conformational flexibility. On the other hand, when the electronic character of the two residues is different (e.g. **4**), the molecules possess a conformational bias, having a preference for folded conformations. These results were corroborated by NOEs and computational modelling. The folded conformation of molecules such as **4** (and others reported previously) may be due to favourably quadrupolar and van der Waals interactions between the unlike aromatic residues. The conformational energies obtained by the ^{1}H NMR analysis of the vicinal coupling constants were used for the calculation of the dipole moments of some molecules (**1**, **3**, **5** and **6**) and excellent agreement with the experimental values was found. Copyright © 2003 John Wiley & Sons, Ltd.
Additional material for this paper is available in Wiley Interscience

KEYWORDS: Arene–arene interactions; conformational analysis; dipole moment; dipole moment; ester; ether; NMR spectroscopy

INTRODUCTION

Non-covalent interactions play key roles in a variety of chemical and physical processes.[1] The interactions of aromatic compounds are ubiquitous in organic chemistry[2] [a comprehensive, updated, list of references on arene interactions (especially CH–π interactions) can be found at: http://www.tim.hi-ho.ne.jp/dionisio/ (last accessed 26 May 2003)]. It has been shown that an aromatic fragment can interact with a variety of chemical entities, such as an other aromatic moiety,[3] hydrogen,[4] cation (for a comprehensive review, see Ref. 5a; for recent reports, see Refs 5b–g), anion,[6] halogen,[7] amide,[8] carbonyl,[9] olefin,[10] electron-donor group[11] or hydrocarbonated fragment.[12] The strengths of these interactions are dependent on the type (intermolecular versus intramolecular), the cooperativity[13] and the relative orientation of the interacting species (for a comprehensive review, see Ref. 14a; for recent reports, see Refs 14b and c). These interactions have profound influences on a wide variety of properties, such as molecular structure,[15] reactivity,[16] supramolecular structure (including molecular recognition[17] and crystal packing[18]), physico-chemical features,[19] biological activity[20] and technological characteristics[21] of organic compounds.

We[22–24] and others[25] have studied the effect of arene–arene interactions on the conformation in solution,[22] the crystal packing[23] and the biological activity[24] of organic molecules. The origin of this phenomenon is not fully understood, although it is likely that dispersion and electrostatic forces dominate the potential of arene–arene interaction. The interpretation of substituent effects can provide valuable insight into the nature of arene–arene interactions and the relative contribution of the different forces.[26]

We have been interested in the synthesis and properties of polymers with aromatic substitution at the ends of an acyclic chain (**A**, Fig. 1).[27] These molecules can be thermotropic liquid crystals,[28] having phase transitions that depend on the flexibility of the acyclic spacer. We

**Correspondence to:* B. Herradón, Instituto de Química Orgánica, CSIC, Juan de la Cierva 3, 28006 Madrid, Spain.
E-mail: herradon@iqog.csic.es
†*Present address:* Schlumberger Oilfield Services, Sugar Land Product Center, 110 Schlumberger Drive, Sugar Land, Texas 77478, USA.
Contract/grant sponsor: Ministerio de Ciencia y Tecnología; *Contract/grant number:* BQU2001-2270.

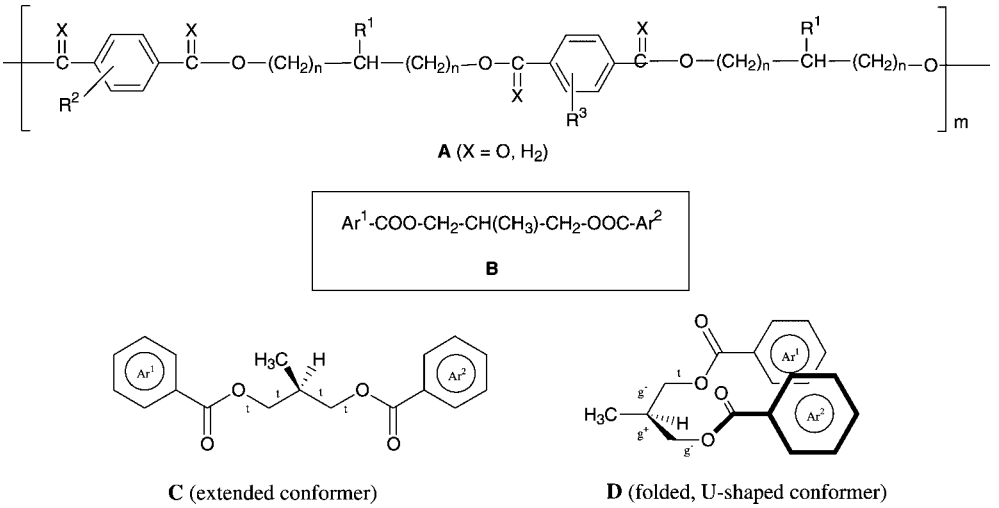

Figure 1. Structures **A**–**D**

hypothesize that the conformational preference of the acyclic spacer of polymers **A** would be controlled by putative intramolecular arene–arene interactions. A convenient approach to obtain an insight into the structure of these polymers is to perform detailed conformational studies on model compounds.[22,27a]

We have recently presented experimental results that show that the conformation of a variety of aromatic diesters of 2-methyl-1,3-propanediol (**B**) depends on the nature of the aryl groups.[22a] Thus, when the aryl groups are identical, the acyclic spacer is quite flexible, with a relatively high content in the extended conformer (**C**). On the other hand, if the electronic character of each aromatic ring is different, the molecules possess a conformational bias, the folded (U-shaped) structure (**D**, Fig. 1) being the most stable conformer. The driving force for this behaviour is an intramolecular interaction between the unlike aromatic rings that is stabilized by both dispersion and quadrupolar forces.[25,29] This intramolecular arene–arene interaction is easy to detect by ^{1}H NMR spectroscopy, and is manifested by a marked asymmetry in the AB parts of the two ABX systems of the spacer and by nuclear Overhauser enhancements between the protons in the two aromatic rings. Occasionally, variations in the chemical shifts of some aromatic protons are observed; this phenomenon depends on the strength of the arene–arene interaction and on the magnetic ring current of each ring. (For recent computational analysis of the chemical shift anisotropy of aromatic compounds, see Ref. 30a; for a comprehensive review, see ref. 30b.)

In continuation of this research, we report here experimental details on the conformational behaviour of several derivatives of 2-methyl-1,3-propanediol (**E**, Fig. 2). The

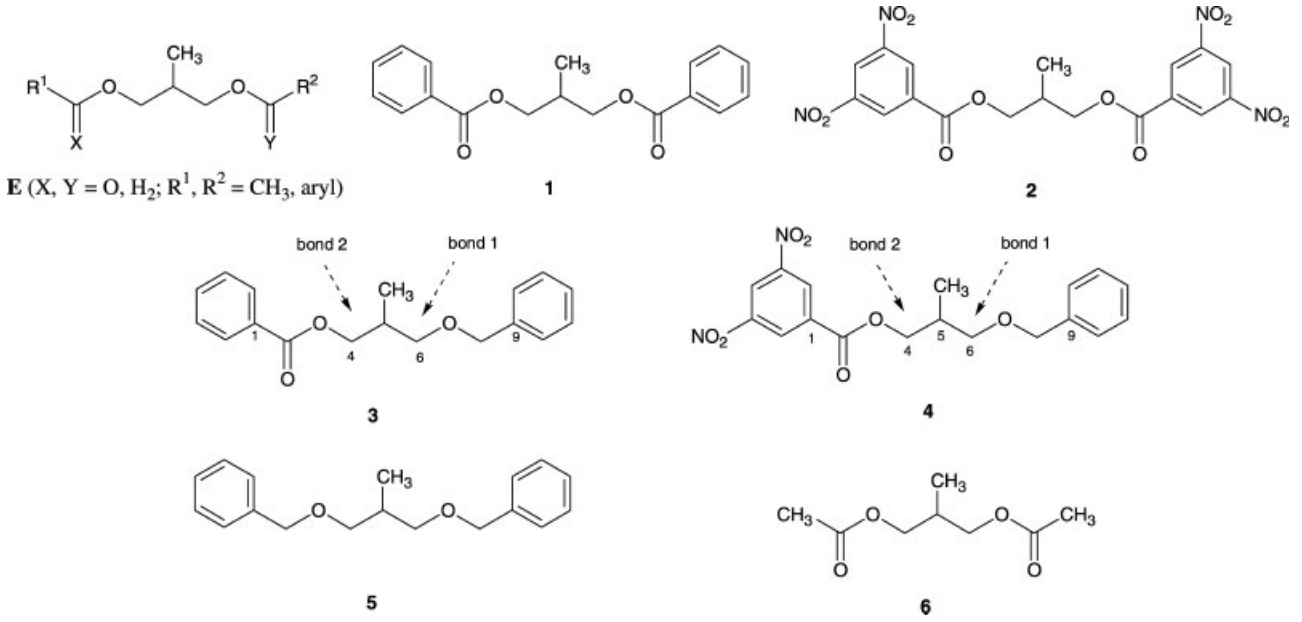

Figure 2. Structures **E** and **1**–**6**

compounds studied possess aromatic rings with different electronic characters. They include diesters (**1** and **2**, Fig. 2), mixed ester–ether compounds (**3** and **4**), and diethers (**5**). The diacetate **6**, without any aromatic fragment, is used as a reference compound to compare experimental data. In previous work,[22a] we dealt only with diesters of 2-methyl-1,3-propanediol; in the present paper, we also report results on the conformation of derivatives of 2-methyl-1,3-propanediol with an ether functionality. Given that both functionalities (ether and ester) are different from both steric and electrostatic points of view, this research can shed light on the relative importance of the different factors influencing the conformation of the functionalized acyclic fragments.

The experimental results were obtained by ^{1}H NMR spectroscopy and dipole moment measurements. We found excellent agreement between the values of conformational energies obtained by the two methods. Additionally, the experimental results were corroborated by computational modelling (both molecular mechanics and *ab initio* calculations). Overall, the results reported in the present paper reinforce our previous findings on the influence of the intramolecular interaction of aromatic rings on the conformation of acyclic molecules, and provide new data on the relative importance of steric and higher order electrostatic interactions.

RESULTS AND DISCUSSION

Analysis of the ^{1}H NMR vicinal coupling constants

In principle, the acyclic spacer of **E** can adopt a variety of conformations, which are generated by rotation around the central bonds. If we consider the rotational isomeric state (RIS) model,[31] the four central bonds in **E** can adopt either *trans* (t), positive *gauche* (g^+) or negative *gauche* (g^-), giving 81 possible limiting conformers. All the structures can be roughly classified as either extended (**C**, Fig. 1) or folded conformations (**D**, Fig. 1). Only four out of the 81 conformers of **E** are U-shaped; these conformers have the $tg^+g^-g^+$, $tg^-g^+g^-$, $g^+g^-g^+t$, and $g^-g^+g^-t$ configurations in the four bonds. Consequently, the spacer in the U-shaped conformers necessarily adopts *gauche* states in the two central bonds, and these conformations can be identified by careful analysis of the proton vicinal coupling constants of the two methylene groups in molecules of type **E**.

Each—$CH_2CH(CH_3)$—segment of **E** gives an ABX system which permits straightforward determination of the vicinal coupling constants, J_{AX} and J_{BX}. Evidently, for the symmetric compounds (**1**, **2**, **5** and **6**), the two ABX systems corresponding to the—$CH_2CH(CH_3)$— and —$CH(CH_3)CH_2$—fragments are identical, whereas in the case of the asymmetric molecules (**3** and **4**), they should yield separate multiplets in the ^{1}H NMR spectra. Figure 3 shows the methylene resonances corresponding

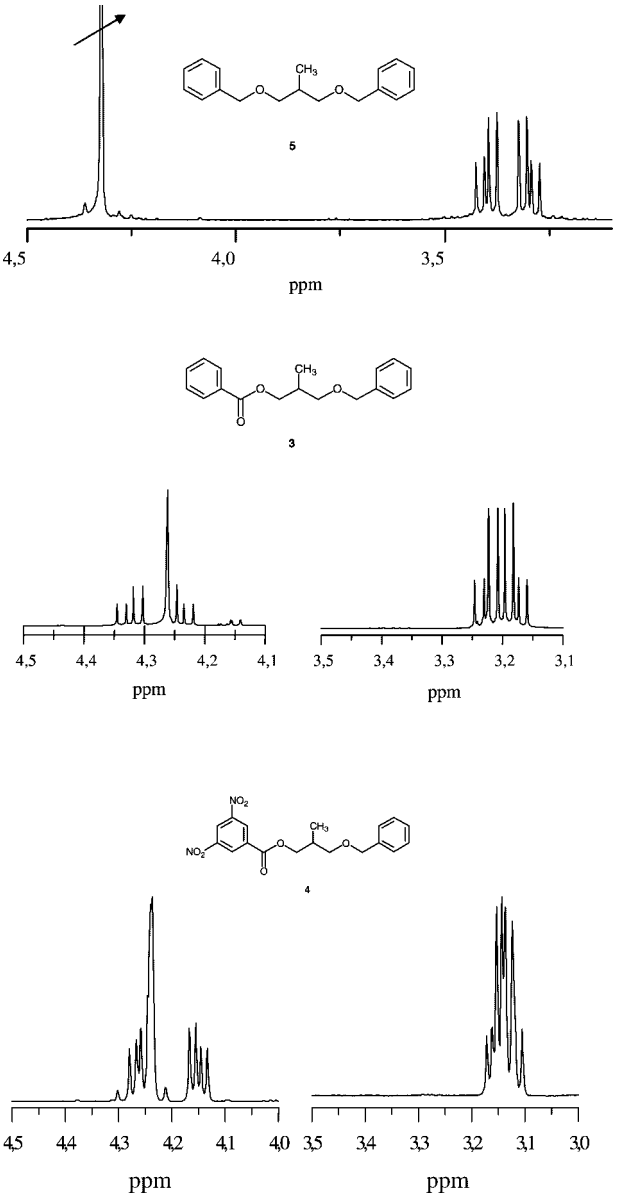

Figure 3. ^{1}H NMR spectral regions of **5** (top), **3** (middle), and **4** (bottom) corresponding to the benzylic protons and the AB parts of the ABX multiplets of the methylene groups. The octuplet at higher field (centred at 3.15–3.25 ppm) is due to the CH_2 group vicinal to the ether function. The octuplet at lower field (centred at ca 4.2 ppm) is due to the CH_2 group vicinal to the ester function. The intense peak at ca 4.25 ppm is from the benzyl methylene. The spectra of **3** and **4** were recorded in benzene-d_6 and that of **5** in dioxane-d_8. All the spectra were taken at 300 MHz and 298 K

to the AB regions of the ABX multiplets for the symmetric diether **5** and the ether–esters **3** and **4**. Each methylene group contributes an octuplet in which the frequencies and relative magnitudes are determined by the chemical shifts (ν_A and ν_B) of the two protons (A and B), the geminal coupling constant (J_{AB}) between them, and the vicinal coupling constants between each of them and the methine (X) proton (J_{AX} and J_{BX}).[32] Although, in general, detailed analysis of second-order spin multiplets requires numerical simulation, we can nevertheless make

some broad comparisons of the different multiplets by visual inspection. In each case, the octuplets may be separated into two quartets which are associated with the two protons, arbitrarily designated A and B. In the following discussion, we adopt the convention that the A spin is that whose chemical shift appears at higher values, so that $\nu_A - \nu_B$ is positive. If the two quartets are approximately symmetrically disposed about the central frequency $(\nu_A + \nu_B)/2$, it follows that the vicinal coupling constants are similar in magnitude. Increasing asymmetry of the two quartets about the central frequency reflects an increasing difference in $|J_{AX} - J_{BX}|$.

Spectra were taken in deuterated benzene at different temperatures (between 298 and 338 K). Since we intended to compare experimental results from ^{1}H NMR spectroscopy and dipole moments, the solvent has to be apolar ($\mu = 0$); although benzene can interact with the aryl groups of compound **E**, this interaction is likely to favour extended versus folded conformations; a computational study on the influence of the solvent on the conformational mobility and other electrostatic properties of molecules of type **E** is under way. The vicinal coupling constants were determined by fitting the lineshapes; a summary of the results is presented in Table 1. The complete set of experimental coupling constants is available as Supplementary Material at the epoc website at http://www.wiley.com/epoc. Owing to the greater relevance of **4**, its coupling constants are given in Table 2.

The relationship between the vicinal coupling constants (J_i^n and $J_i^{n\prime}$, for the two bonds $n = 1$, 2) and conformation is depicted in Fig. 4, which shows the projections for each of the rotational isomeric states of the two central C—C bonds of the 2-methyl-1,3-propanedioxy spacer common to all the compounds studied. The protons have been arbitrarily labeled *a* and *b* for the methylene group of bond 1, *c* and *d* for the methylene group of bond 2 and *x* for the methine group to which they couple. On the basis of symmetry grounds, the two bonds in **1**, **2**, **5**, and **6** are energetically equivalent, which implies that the g^+ state of bond 1 is equivalent to the g^- state of bond 2 and has equal energy. As a convention, for the asymmetric compounds **3** and **4**, we name methylene group 1 as the one that appears at higher field (i.e. the vicinal to the ether functionality) and the methylene group 2 as the one vicinal to the ester function. Note that no assignment has yet been made regarding the chemical shifts of these protons in any of the compounds. Thus the downfield A spin quartets could correspond to proton *a* or *b* in the case of methylene group 1. Similarly for the methylene group 2, which shows different multiplets in the asymmetric compounds **3** and **4**, the higher frequency resonances A may derive from either proton *c* or *d*.

Equations (1)–(4) relate the vicinal coupling constants J_{ax}, J_{bx}, J_{cx} and J_{dx} with the populations $f_{(t)}^n$, $f_{(+)}^n$ and $f_{(-)}^n$

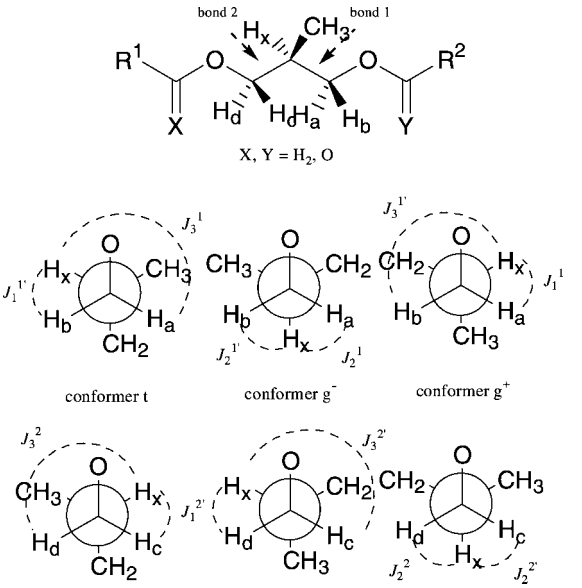

Figure 4. Projections showing the conformation-dependent coupling constants, J_i^n and $J_i^{n\prime}$ (for the two bonds $n = 1$, 2), between methylene and methyne protons in the central C—C bonds of the 2-methyl-1,3-propanedioxy spacer common to all the compounds studied Projections are shown for bonds 1 and 2, which are mirror images in the symmetric compounds

Table 1. Range of the temperature-dependent coupling constants for the ABX system of compounds **1**–**6**[a]

Compound	J_{AX}	J_{BX}
Dibenzoate (**1**)	6.41–6.53	5.57–5.74
Bis[3,5-(dinitro) benzoate] (**2**)	6.47–6.52	5.62–5.66
Benzoate, benzyl ether (**3**)	6.18–6.28 (bond 1)	5.63–5.64 (bond 1)
	6.12–6.16 (bond 2)	6.03–6.08 (bond 2)
Benzyl ether, [3,5-(dinitro)benzoate] (**4**)	6.65–6.85 (bond 1)	4.82–5.08 (bond 1)
	6.34–6.36 (bond 2)	5.90–5.97 (bond 2)
Diether (**5**)	6.02–6.07	5.88–5.89
Diacetate (**6**)	6.41–6.46	5.75–5.82

[a] Bonds **1** and bond **2** of **3** and **4** are indicated in Fig. 2. All the spectra, except for the diether **5**, were measured in benzene-d_6; the spectra of **5** were taken in dioxane-d_8. The spectra were recorded between 298 and 338 K.

Table 2. Coupling constants (Hz) for compound **4**

Parameter	298 K	300 K	303 K	308 K	313 K	323 K	338 K
Bond 1: J_{AX}	6.85	6.81	6.79	6.79	6.75	6.71	6.65
Bond 1: J_{BX}	4.82	4.86	4.86	4.90	4.88	4.88	5.08
Bond 2: $J_{A'X}$	6.36	6.36	6.36	6.35	6.35	6.35	6.34
Bond 2: $J_{B'X}$	5.90	5.91	5.91	5.92	5.93	5.95	5.97

of the t, g^+, and g^- states for bonds $n = 1, 2$. Equation (5) shows the relationship between the population and the energy of each of the three conformational states μ for each bond n.[22a]

$$J_{ax} + J_{bx} = J_3^1 + J_1^1 - f_{(-)}^1\left(J_3^1 + J_1^1 - 2J_2^1\right) \quad (1)$$

$$J_{ax} - J_{bx} = (J_3^1 - J_1^1)\left[f_{(t)}^1 - f_{(+)}^1\right] \quad (2)$$

$$J_{cx} + J_{dx} = J_3^2 + J_1^2 - f_{(+)}^2\left(J_3^2 + J_1^2 - 2J_2^2\right) \quad (3)$$

$$J_{cx} - J_{dx} = \left(J_1^2 - J_3^2\right)\left[f_{(t)}^2 - f_{(-)}^2\right] \quad (4)$$

$$f_{(v)}^n = \frac{\exp\left(-E_{(v)}^n/RT\right)}{\sum_\mu \exp\left(-E_{(\mu)}^n/RT\right)} \quad (5)$$

These quantities may be compared with the experimental quantities, $J_{AX} + J_{BX} = J_{ax} + J_{bx}$ and $|J_{AX} - J_{BX}| = |J_{ax} - J_{bx}|$ for both bonds. As inferred from the data in Table 1, the vicinal coupling constants for **1**, **2**, **3**, **5** and **6** are similar with $J_{AX} + J_{BX} \approx 12$ Hz and a small value of $|J_{AX} - J_{BX}|$ (<1 Hz), which suggests that the conformational distributions for all the compounds are very similar, determined presumably by the same interactions within the chain. On the other hand, the $|J_{AX} - J_{BX}|$ values for the more shielded methylene group of **4** goes from 1.6 to 2.0 Hz over the temperature range studied (Table 2). This indicates that the two protons of the methylene group 1 in **4** sample very different average environments, which results in biased population distributions between the *trans*, *gauche*(+) and *gauche*(−) states of the central C—C bonds of the acyclic spacer.

Following previously published methodology,[22a] we can estimate the energies of the *gauche* states relative to the *trans* state (i.e. $E_{(t)}^n = 0$ of the central bonds in all the molecules **1**–**6**). The results are given in Table 3. Note that for the symmetrical compounds (**1**, **2**, **5** and **6**), the energies given refer to bond 1. For bond 2, the *gauche* energies, $E_{(+)}$ and $E_{(-)}$, are interchanged. In the case of the asymmetric compounds (**3** and **4**), results for bond 1 (vicinal to the ethereal oxygen) and bond 2 (vicinal to the ester function) are given in Table 3.

Table 3. Average conformational energy values for compounds **1**–**6**[a]

Compound	$E_{(+)}$ (J mol^{-1})	$E_{(-)}$ (J mol^{-1})
1	-800 ± 400	-400 ± 300
2	-900 ± 300	-200 ± 150
3[b]	-700 ± 200	-500 ± 200
3[c]	-300 ± 200	-100 ± 100
4[b]	-2000 ± 500	-1000 ± 1000
4[c]	-600 ± 200	-500 ± 200
5	-150 ± 100	300 ± 150
6	-700 ± 200	-450 ± 150

[a] The data are relative to the energy of the *trans* conformer. The data are for benzene-d_6 solution, except those for **5**, which are for dioxane-d_8 solution.
[b] The data are for bond 1 (see Fig. 2).
[c] The data are for bond 2 (see Fig. 2).

On the basis of the data reported above, it is clear that the conformational distribution of the ether–ester **4** is different that of the rest of the molecules. Whereas **1**–**3**, **5** and **6** have a relatively high conformational flexibility in the two central bonds of the spacer, **4** shows a conformational bias, with a *gauche*-preferred conformation at the bond between the more shielded CH_2 group (vicinal to the ethereal oxygen) and the central bond. It is also worth mentioning that the mean chemical shift for the CH_2 group vicinal to the ethereal oxygen shows a significant difference: 3.34 ppm for diether **5**, 3.20 ppm for **3**, and 3.09 ppm for the dinitro derivative **4**. The shielding of this methylene can be rationalized by its proximity to the aromatic ring at the other end of the molecule; this effect is greatly manifested in **4** and, to a lesser extent, in the benzoate **3**.

Overall, we can state that the conformational distribution of the acyclic linker in **4** is different from the rest of the related molecules analogous molecules. Based on previous findings,[22a] we can propose that the most stable conformations of **4** are folded (U-shaped). This hypothesis was confirmed by NOE experiments and computational modelling.

NOE measurements and computational modelling

In order to confirm further the existence of folded conformer(s) of **4**, 1D-NOE experiments were performed, in C_6D_6 solution, by using the double pulse field gradient spin-echo (DPFGSE) sequence.[33] The aromatic protons in both the dinitrophenyl and the phenyl rings and also the methylene protons on bond 1 were chosen as targets and thus selectively inverted.

The theory of transfer of magnetization under transient NOE conditions is well known[34] and will not be given here. The protocol to derive proton–proton distances from these experiments can be found elsewhere.[22a] Different NOE mixing times were used after inversion of the target protons and both the recovery of the magnetization of the inverted proton and the build-up of the NOEs on the neighbouring protons were considered. It was observed that the inversion of the *ortho*-protons of the 3,5-dinitrophenyl ring produced clear positive NOE enhancements on the aromatic protons of the phenyl ring and also on all the aliphatic methine, methylene and methyl groups (Fig. 5, top). Analogously, inversion of the aromatic protons of the phenyl ring gave rise to NOE enhancements on the *ortho*-protons of the dinitrophenyl ring (not shown). In contrast, no inter-ring enhancements were observed upon inversion of the

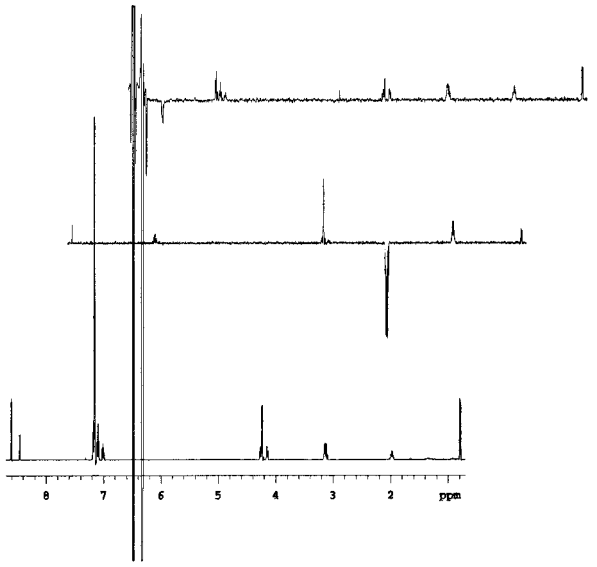

Figure 5. 1D-NOE spectra obtained upon inversion of the *ortho*-protons of the dinitrophenyl group of **4** (top) and of the methylene protons vicinal to the ether group of the same compound (middle). The regular 500 MHz ^{1}H NMR 1D spectrum is shown at the bottom. The mixing time was 1.0 s

para-proton of this dinitrophenyl ring. In addition, inversion of the methylene protons on bond 1 gave rise to similar enhancements on both the aromatic protons of the phenyl ring and on the *ortho*-protons of the dinitrophenyl ring (Fig. 5, middle). Obviously, since NMR-derived data are time-averaged, the observed enhancements reflect the conformational equilibrium which is present in solution. Therefore, the fact that cross-relaxation between protons belonging to the two aromatic rings takes place indicates unambiguously that an appreciable percentage of folded (U-shaped) conformers exist in solution, since for extended conformers, both aromatic rings would be far apart. The corresponding average interproton distances, estimated from the NOE build-up curves, are given in Table 4.

In order to obtain a reasonable structure that could fit the NMR-derived data, a computational study on the conformational distribution of **4** was performed. Initially a molecular mechanics based conformational search was chosen owing to its shorter computation time compared with quantum calculations. Molecular mechanics calculations were performed using the MM3* force field as implemented in MacroModel 4.5 (Columbia University, 1994).[35] A systematic search of the low-energy conformers was performed by using the MULTIC facility of the MacroModel software. Thus, the six torsion angles that connect both aromatic rings were systematically varied in 120° steps to cover the possible staggered conformers. In total, 729 conformers were generated and optimized using 200 steepest descent steps, followed by the number of conjugate gradient iterations required for complete convergence. An effective dielectric constant $\varepsilon = 1$ was used. Only nine different conformers occurred within an energy threshold of 25 kJ mol^{-1}. (The resulting structures, their torsion angles and relative energies are given in the Supplementary Material available at the epoc website on Wiley Interscience). However, this study gave an overwhelming preponderance of folded conformations that was unrealistic. This result was not unexpected given that molecular mechanics calculations on aromatic compounds are known to favour stacked structures overestimating the importance of van der Waals interactions.[36] In order to overcome this drawback, we carried out a conformational *ab initio* study on **4**.

Table 4. Estimated average interproton distances[a] between protons on opposite sides of ether–ester **4**[b]

Proton pair	Distance (nm)	Proton pair	Distance (nm)
o-DNP/*o*- and *m*-Ph	0.41	*p*-DNP/*o*- and *m*-Ph	>0.5[c]
A-CH_2/*o*- and *m*-Ph	0.31	A-CH_2/*o*-DNP	0.33
A-CH_2/B-CH_2	0.26		

[a] Calculated from $\left(6\sqrt{\left\langle r_{ij}^{-6}\right\rangle}\right)^{-1}$.

[b] Estimated errors are below 10%. In the case of the methylene groups, both protons were simultaneously inverted. DNP and Ph are the 3,5-dinitrophenyl and the phenyl groups, respectively. The methylene group A is vicinal to the benzyloxy group (bond 1) and the methylene group B is vicinal to the 3,5-dinitrobenzoyloxy group (bond 2) (see Fig. 2).

[c] NOE is not observed.

All the *ab initio* computations were performed under vacuum (effective dielectric constant $\varepsilon = 1.0$). The starting geometries for the calculations were generated through a conformational search using a Monte Carlo algorithm[37] with 5000 steps and the AMBER force field.[38] The resulting conformations were analysed on the basis of their energy content, discarding those conformations that were 80 kJ mol^{-1} over the most stable structure. Overall, 57 conformations were obtained that were classified in two families: folded (42 structures) or extended (15 structures). The structural variations among the conformer of each family were small. The dihedral angles of the linker in the folded family were very similar and only small differences in the relative position of the centres of the two aromatic rings were observed. Interestingly, the relative orientation of the two aromatic rings was face to face in all the folded conformers, and T-shaped structures (likely to be stabilized by CH–π interactions[12]) were not detected, probably hampered by the short length of the spacer. On the other hand, a higher structural variability was observed in the family of extended conformers, arising from small differences in the dihedral angles in the acyclic spacer and more significant variations in the rotation around the Ph—CH_2 bond. Although of limited value, it was found that the most stable folded conformer was more stable than the most stable extended conformer (ca 19 kJ mol^{-1}).

The structures of the most stable conformer in each family were further refined by the B3LYP hybrid Hartree–Fock/density functional method[39] using the

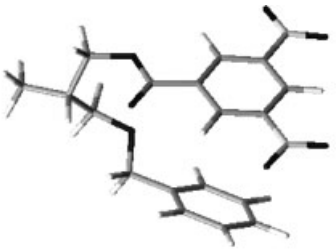

Folded conformer (E = -1332.66057 Hartrees)

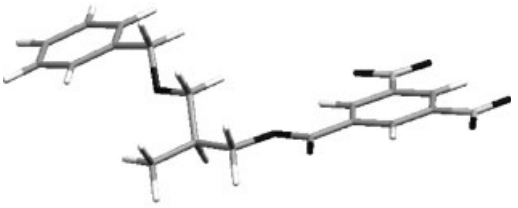

Extended conformer (E = -1332.63522 Hartrees)

Figure 6. Optimized calculated (B3LYP/6–31G*) structures for the folded and the extended conformers of compound **4**

6–31G* basis set as implemented in the Gaussian 98 programs.[40] The calculations were carried out at high convergence and the resulting structures were characterized by harmonic vibrational frequency computation that showed that the structures were minima on the potential energy surface. The resulting structures, along with their respective energies, are shown in Fig. 6 (the atomic coordinates of the optimized *ab initio* structures for the folded and extended conformers are included as Supplementary Material); they were not very different from the structures obtained by the Monte Carlo method (the superposition of the Monte Carlo and *ab initio* structures for the folded and extended conformers are included as Supplementary Material, available at the epoc website on Wiley Interscience). The calculation indicated that the folded conformer is more stable than the extended conformer; the energy difference is 0.025 hartree (ca 66 kJ mol^{-1}), which is much higher than the experimental value, although it must be remarked that the computations were done under vacuum and the experimental results were obtained in benzene solution.

From a geometric point of view, the folded structure fits the experimental facts fairly well. The most significant aspect is the comparison of the experimental and computed values of the distance between the *ortho*-protons of the dinitrophenyl ring and the *ortho*-protons of the phenyl ring: 0.41 nm (experimental), 0.32 nm (shortest distance in the computed folded conformer with 0.48 nm as average distance) and 0.65 nm (shortest distance in the computed extended conformer with 0.80 nm as average distance).

As a conclusion, the predominant presence of folded conformers is confirmed by both the calculations and the NOE experiments, indicating that folded type conformations such as the minimum indicated in Fig. 6 and related structures arising from small changes in the torsion angles in the linker are significantly present in the conformational equilibrium.

Dipole moment measurements

Compounds of type **E** (Fig. 2) are convenient models for oligomers and polymers with aromatic residues linked by an acyclic spacer. The conformational analysis of polymers and model compounds through the study (theoretical and experimental) of dipole moments is a frequent methodology in the field of the chemical physics of polymers. Another goal of the present research was to compare data obtained by ^{1}H NMR spectroscopy and dipole moment measurements in the conformational analysis of compounds **E**.

The flexibility of the spacer in the molecules of type **E** can be expressed in terms of its rotational partition function Z given by the equation

$$Z = \mathbf{J}^* \left[\prod_{i=2}^{n-1} \mathbf{U}_i \right] \mathbf{J} \tag{6}$$

where $\mathbf{U}_i$ is the matrix that embodies the statistical weights or Boltzmann factors, σ, of the rotational states of the bonds i that are related to the conformational energies, E, of these states by Eqn (7), where the subscripts η and ζ indicate the rotational states of bond i and $i-1$, respectively.

$$\sigma_{\zeta\eta} = \exp\left(-\frac{E_{\zeta\eta}}{RT}\right) \tag{7}$$

$\mathbf{J}* = (1, 0, \ldots, \nu, \ldots 0)$ and $\mathbf{J} = (1, 0, \ldots \nu, \ldots 0)$ in Eqn (6) are the row vector ($1 \times \nu$) and the column vector ($\nu \times 1$), respectively, where ν is the number of rotational states. By normalizing to the unit the higher statistical weight of the rotational states of each skeletal bond, a value is obtained for the rotational partition function, which is straightforwardly related to the flexibility of the spacer. The flexibility can alternatively be expressed by the conformational entropy, which is related to the partition function by the equation

$$S_c = \frac{R}{n}\left(\ln Z + \frac{T}{Z}\frac{\mathrm{d}\log Z}{\mathrm{d}\log T}\right) \tag{8}$$

where n is the number of skeletal bonds of the spacer and T is the absolute temperature.

According to the rotational isomeric state (RIS) model,[31,41] a conformation-dependent property $< X >$

(such as the mean-square dipole moment $<\mu^2>$) can be calculated by

$$\langle X\rangle = Z^{-1}\prod_{i=1}^{n}\mathbf{X}_i \tag{9}$$

where $\mathbf{X}_i$ is a supermatrix that contains the appropriate statistical-weight matrix $\mathbf{U}_i$, a coordination transformation matrix $\mathbf{T}_i$ and the specific contribution of bond i to the property X.

The location of the rotational states and the establishment of their relative energies are obtained, whenever possible, from spectroscopic or thermodynamic measurements carried out on molecules having structural features similar to those of the spacer. When the experimental option is not possible, computational methods are used.

In the previous section, we calculated the conformational energies for the two central bonds of the spacer of **1**–**6** by analysis of the ^{1}H NMR vicinal coupling constants. The values of the conformational energies of **1**, **3**, **5** and **6** were used for the theoretical calculation of their mean-square dipole moments and, therefore, the reliability of the method based on ^{1}H NMR spectroscopy can be tested by comparing the experimental and theoretical dipole moments. The theoretical mean-square dipole moments of the nitro-substituted compounds **2** and **4** were not calculated as there are no reliable data on the contribution of the nitro group to the overall dipole moment of a molecule. However, as **4** has interesting conformational properties, the experimental value of its dipole moment was also determined (see below).

All the background on the theoretical calculation of dipole moments has been extensively discussed in other publications;[27a,41] the details will not be repeated here and just a brief outline follows.

For compounds of type **E**, the dipole moment associated with an ester group, μ_E, is assumed to be located in the (O)C—O bond, forming an angle of 123° with the CH_3—C(O) or the C^{arom}—C(O) bonds of the aliphatic and aromatic esters, respectively. The values of μ_E are 1.75 and 1.89 D (1 D = 10^{-18}esu cm) for the former and latter esters, respectively. The dipole moments of an ether group lies along the bond and their values are μ(O—CH_2) = $-\mu$(CH_2—O) = 1.07 D. The dipole moments for the other bonds (C—C) are considered to be zero. The rotational angles are assumed to be located at 180° (*trans*) or ±60° (*gauche* states), with the exception of the O—C(O) bonds, which are restricted to *trans* states, and the O—CH_2 of the ester moiety, located at 180 and ±76°, respectively.

The rotational states of positive sign about these bonds have an energy $E_{\sigma k} = 1.67\,\mathrm{kJ\,mol^{-1}}$ above that of the alternative *trans* states. However, the g^- states give rise to strong repulsive interactions between the methyl and the carbonyl groups. The energies of these states are $E_{\sigma k} + E_w$, where E_w ($= 5.86\,\mathrm{kJ\,mol^{-1}}$) is the second-order energy between the carbonyl and the methylene groups. The *gauche* states of positive sign (+120°) about bonds of type 2 (−120° about bonds of type 1, see Fig. 2) place the oxygen atom between the methyl and the methylene groups, causing stronger repulsive interactions than the alternative *gauche* states (−120°) where the methyl group is located in the plane and the methylene group is out of the plane, that is, they interchange their locations. The energy associated with the g^+ and the g^- rotational states will be denoted $E_{\sigma\beta}$ and $E_{\sigma\alpha}$, respectively, and they were determined by ^{1}H NMR spectroscopy as described above. Finally *gauche* rotations about the ethereal CH_2—O bonds, which give rise to first-order CH···O interactions, have an energy $E_{\sigma'}$ of ca $3.8\,\mathrm{kJ\,mol^{-1}}$ above that of the *trans* states. Rotational states of different sign about two consecutive bonds, which give rise to second-order interactions between a methylene (or methyl) group and the carbonyl group, have an energy, E_w, of $\sim 5.86\,\mathrm{kJ\,mol^{-1}}$ above that of the tt states. Rotations of type g^-g^+ about bonds that produce second-order interactions between two oxygen atoms or between an oxygen atom and a methylene group separated for four bonds have in both cases an energy, E_w, of $\sim 2.5\,\mathrm{kJ\,mol^{-1}}$ above that of the alternative tt states.

The statistical weight matrices for the different skeletal bonds of the diesters **1** and **6** have been reported previously.[27a] The statistical weight matrices for the different skeletal bonds of the diether derivative **5** can be written as

$$\mathbf{U}(\mathrm{O{-}C_4}) = \begin{pmatrix} 1 & \sigma' & 0 \\ 0 & \sigma' & 0 \\ 1 & 0 & 0 \end{pmatrix}; \qquad \mathbf{U}(\mathrm{C_4{-}C_5}) = \begin{pmatrix} 1 & \sigma_\beta & \sigma_\alpha \\ 1 & 0 & 0 \\ 0 & 0 & \sigma_\alpha \end{pmatrix};$$
$$\mathbf{U}(\mathrm{C_5{-}C_6}) = \begin{pmatrix} 1 & \sigma_\alpha & \sigma_\beta \\ 1 & \sigma_\alpha & w\sigma_\beta \\ 1 & w\sigma_\alpha & \sigma_\beta \end{pmatrix}; \qquad \mathbf{U}(\mathrm{C_6{-}O}) = \begin{pmatrix} 1 & \sigma' & 0 \\ 1 & \sigma' & 0 \\ 1 & 0 & 0 \end{pmatrix} \tag{10}$$

where σ and w are first- and second-order statistical weight parameters, respectively. Correspondingly, for **3**, having ester and ether functionalities, the statistical weight matrices can be written as (see overleaf).

Matrix multiplication methods,[41] were used to calculate the mean-square dipole moments of the compounds and the results obtained are given in Table 5. By comparing the experimental and theoretical values of $<\mu^2>$, it

$$\mathbf{U}(\mathrm{O{-}C_4}) = (1 \quad \sigma_k \quad \sigma_k w_k); \qquad \mathbf{U}(\mathrm{C_4{-}C_5}) = \begin{pmatrix} 1 & \sigma_\beta & \sigma_\alpha \\ 1 & w_k\sigma_\beta & w_k\sigma_\alpha \\ 1 & w_k\sigma_\beta & \sigma_\alpha \end{pmatrix};$$

$$\mathbf{U}(\mathrm{C_5{-}C_6}) = \begin{pmatrix} 1 & \sigma_\alpha & \sigma_\beta \\ 1 & \sigma_\alpha & w\sigma_\beta \\ 1 & w\sigma_\alpha & \sigma_\beta \end{pmatrix}; \qquad \mathbf{U}(\mathrm{C_6{-}O}) = \begin{pmatrix} 1 & 0 & \sigma'' \\ 1 & \sigma'' & 0 \\ 1 & 0 & 0 \end{pmatrix} \tag{11}$$

Table 5. Results of the dielectric measurements of compounds **1** and **3–6**

Compound	Solvent	$\left(\frac{\partial\varepsilon}{\partial w_2}\right)^\circ$	$2n_1\left(\frac{\partial n}{\partial w_2}\right)^\circ$	$<\mu^2>_{\mathrm{exp}}$ (D^2)	$<\mu^2>_{\mathrm{theor}}$ (D^2)
1	Benzene	2.24	0.11	5.90	5.86
3	Benzene	1.71	0.11	4.32	5.35
4	Benzene	4.82	0.13	16.69	n.d.
5	Dioxane	1.48	0.31	2.62	2.64
6	Benzene	3.16	0.29	4.76	4.95

can be seen that the values of the conformational energies determined from ^{1}H NMR experiments carried out on the dibenzoate **1**, the diether **5** and the diacetate **6** reproduce very satisfactorily the mean-square dipole moments of these compounds. On the other hand, the calculated value for the mixed ether–ester **3** is nearly 24% higher than the experimental result. To fit the calculated and experimental values of $<\mu^2>$ for **3** would require favouring the all-*trans* conformation which places the dipole moments associated with the ester and ether groups in nearly antiparallel orientations. The experimental value of the mean-square dipole moment of the dinitrobenzoyl derivative **4** is also included in Table 5; it is much higher than for the other model compounds, which may reflect the high contribution of the nitro group to the overall dipole moment of the molecule and also the higher proportion of folded conformations in the overall conformational distribution of this molecule.

CONCLUSIONS

The experimental results (^{1}H NMR and dipole moments) for derivatives of 2-methyl-1,3-propanediol having aromatic rings at the ends of the acyclic chain have shown that the conformation of the spacer depends on the nature of the aromatic rings. Thus, whereas the dinitrobenzoyl derivative **4** has a preference for folded (U-shaped) conformers, the rest of the molecules studied have a higher conformational mobility with a likely preference for extended structure.

The conformational behaviour of these compounds can be explained by quadrupolar interactions between the aromatic rings. The conformational bias of **4** can be attributed to favourable quadrupolar interactions between the 3,5-dinitrobenzoyl and phenyl groups at the ends of the molecule; this conformation is also favoured by van der Waals interactions. On the other hand, the fact that the other compounds (**1–3** and **5**) have a lower population of the folded conformer can be rationalized by a destabilizing quadrupolar interaction between the two aromatic rings, that tend to place the aromatic fragments apart from each other (as previously found in the solid state[23a]), although a face-to-face orientation is preferred by van der Waals forces.

It is worth highlighting that the conformational energies obtained by ^{1}H NMR spectroscopy were used to calculate the dipole moments of **1**, **3**, **5** and **6**, showing agreement with the experimental values, which indicates a good validation of the method based on ^{1}H NMR spectroscopy.

We have previously found a similar behaviour in the conformational preferences of 1-(9-anthracenecarbonyloxy)-3-(3,5-dinitrobenzoyloxy)-2-methylpropane (**7**),[22a] which shows a very high preference for folded conformations (over 90% of the conformational distribution), presenting U-shaped conformations with a nearly perfect alignment of the mass centres of the two aromatic rings (Figure 7); this conformation maximizes the (favourable) quadrupolar interaction between the two unlike aromatic rings. As a consequence, the *gauche* states for the two central bonds of **7** are highly populated, with an energy difference of over 5 kJ mol^{-1} relative to the *trans* states. The same phenomenon, although to a smaller extent, is

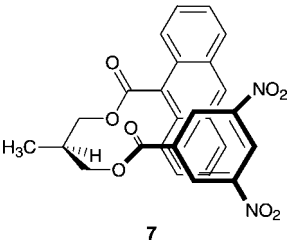

7

Figure 7. Structure **7**

found with **4**. On the other hand, the stabilizing energy of the *gauche* states of the central bonds in **4** (ca 2 kJ mol^{-1}) is lower, indicating a decrease in the *gauche* population in **4** relative to **7**, resulting in a lower proportion of U-conformer in **4** than in **7**. This result is expected on the basis of the higher absolute value of the *zz*-component of the quadrupole moment tensor of anthracene relative to that of benzene[42] that would result in smaller quadrupolar interaction energy for **4**. Another reason for a lower proportion of the U-shaped conformer in **4** may be due to the unfavourable steric interaction of the benzylic methylene (see the structure of the folded conformer in Fig. 6).

In conclusion, the present and our previous results demonstrate that the conformation of acyclic spacers bearing aromatic substituents can be controlled by the proper choice of the electrostatic character of the aromatic rings and the functionality at the end of the acyclic spacer. These results can be applied to the preparation of oligomers and polymers with designed folding patterns. Work along these lines is in progress.

EXPERIMENTAL

Materials. All compounds were prepared using standard methodologies (acylation with the corresponding acyl chloride or alkylation with benzyl bromide) from 2-methyl-1,3-propanediol, following procedures reported in the literature.[22,23a] All the new compounds gave satisfactory ^{1}H NMR spectra, ^{13}C NMR spectra, mass spectra and analytical data (C, H, ±0.4%).

NMR measurements. ^{1}H NMR spectra were recorded on INOVA 300, INOVA 400 and UNITY 500 spectrometers. All the spectra, except those of **5**, were obtained in benzene-d_6 solutions. The ^{1}H NMR spectra of **5** were obtained in dioxane-d_8. Coupling constants were determined by fitting the experimental spectra with simulated lineshapes based on standard expressions for the line frequencies for ABX spin systems.[32] A FORTRAN program was developed for this purpose that employs a non-linear least-squares fitting routine in which the chemical shifts and respective linewidths for spins A, B and X, and also the geminal and vicinal coupling constants, are varied simultaneously. Errors in the coupling constants determined in this way are less than 0.05 Hz in all cases. All spectra were measured between 298 and 338 K. Transient NOE measurements were performed on a Varian Unity 500 spectrometer at 303 K in benzene-d_6 solution, using standard procedures. Five mixing times (0.3, 1.0, 2.0, 3.0 and 6.0 s) were employed to follow the build-up and decays of NOEs.

Computational modelling. The calculations were performed on a double 867 MHz processor PC and on a 2660 MHz Intel Xeon processor (Xeon) Dell Precision 450 workstation running both Linux and Microsoft Windows XP (version 2002) operating systems.

Dipole moments. The static dielectric permittivities ε of solutions of **1**, **3**, **4** and **6** were measured in benzene (Merck, dried with molecular sieves) at 303 K with a capacitance bridge (General Radio, type 1620 A) coupled with a three-terminal cell. Owing to its limited solubility in benzene, the dielectric measurements of the diether **5** were obtained in dioxane (Panreac) solution that was dried by sequential heating at reflux over potassium hydroxide and methyl isocyanate to eliminate the presence of aldehydes and alcohols. The values of ε were plotted against the weight fraction w of solute, and from the slope of the plots, in the limit $w \to 0$, the term dε/dw, proportional to the total polarization (orientation, electronic and atomic), was obtained. Values of the increment of the refractive index n of the solutions with respect to that of the solvent n_1 were measured with a differential refractometer (Chromatix). The values of Δn were plotted against w, and from the slope in the limit $w \to 0$, the term dn/dw, proportional to the electronic polarization, was determined. The atomic polarization is in most cases only a very small percentage of the electronic polarization and because of the small value of the latter, this contribution was neglected. The mean-square dipole moments of the compounds were obtained by using the Guggenheim–Smith method:[41]

$$< \mu^2 >= \frac{27\, k_B T M_0}{4\pi\rho N_A (\varepsilon_1 + 2)^2} \lim_{w\to 0}\left[\left(\frac{\partial\varepsilon}{\partial w}\right)^{\circ} - 2n_1\left(\frac{\partial n}{\partial w}\right)^{\circ}\right] \quad (12)$$

where k_B and N_A are Boltzmann's constant and Avogrado's number, respectively, M_0 is the molecular weight of the solute, T is the absolute temperature, ρ is the density of the solvent and n_1 and ε_1 are the refractive index and the permittivity of the solvent, respectively.

Acknowledgement

P. B. thanks the CAM for a postdoctoral fellowship.

REFERENCES

1. (a) Rigby M, Smith EB, Wakeham WA, Maitland GC. *The Forces Between Molecules*. Clarendon Press: Oxford, 1986; (b) Stone AJ. *The Theory of Intermolecular Forces*. Clarendon Press: Oxford, 1996.
2. Hunter CA, Lawson KR, Perkins J, Urch CJ. *J. Chem. Soc., Perkin Trans. 2* 2001; 651–669.
3. (a) Hunter CA, Sanders JKM. *J. Am. Chem. Soc.* 1990; **112**: 5525–5534; (b) Luhmer M, Bartik K, Dejaegere A, Bovy P, Reise J. *Bull. Soc. Chim. Fr.* 1994; **131**: 603–606; (c) Hobza P, Selzle HL, Schlag EW. *J. Am. Chem. Soc.* 1994; **116**: 5300–5306.

4. (a) Rozas I, Alkorta I, Elguero J. *J. Phys. Chem. A* 1997; **101**: 9457–9463; (b) Harder S. *Chem. Eur. J.* 1999; **5**: 1852–1861; (c) Scheiner S, Kar T, Pattanayak J. *J. Am. Chem. Soc.* 2002; **124**: 13257–13264.
5. (a) Ma JC, Dougherty DA. *Chem. Rev.* 1997; **97**: 1303–1324; (b) Cubero E, Luque FJ, Orozco M. *Proc. Natl Acad. Sci. USA* 1998; **95**: 5976–5980; (c) Choi HS, Suh SB, Cho SJ, Kim KS. *Proc. Natl Acad. Sci. USA* 1998; **95**: 12094–12099; (d) Gokel GW, De Wall SL, Meadows ES. *Eur. J. Org. Chem.* 2000; 2967–2978; (e) Meadows ES, De Wall SL, Barbour LJ, Gokel GW. *J. Am. Chem. Soc.* 2001; **123**: 3092–3107; (f) Beene DL, Brandt GS, Zhong W, Zacharias NM, Lester HA, Dougherty DA. *Biochemistry* 2002; **41**: 10262–10269; (g) Bartoli S, Roelens S. *J. Am. Chem. Soc.* 2002; **124**: 8307–8315.
6. (a) Alkorta I, Rozas I, Elguero J. *J. Am. Chem. Soc.* 2002; **124**: 8593–8598; (b) Quiñoñero D, Garau C, Rotger C, Frontera A, Ballester P, Costa A, Deyá PM. *Angew. Chem., Int. Ed. Engl.* 2002; **41**: 3389–3392.
7. (a) Thalladi VR, Weiss HC, Bläser D, Boese R, Nangia A, Desiraju GR. *J. Am. Chem. Soc.* 1998; **120**: 8702–8710; (b) Legon AC. *Chem. Eur. J.* 1998; **4**: 1890–1897.
8. (a) Ganis P, Valle G, Pandolfo L, Bertani R, Visentin F. *Biopolymers* 1999; **49**: 541–549; (b) Duan G, Smith VH Jr, Weaver DF. *Chem. Phys. Lett.* 1999; **310**: 323–332.
9. Wormald J. *Fluid Phase Equilibria* 1997; **133**: 1–10.
10. Mulzer J, Schein K, Böhm I, Trauner D. *Pure Appl. Chem.* 1998; **70**: 1487–1493.
11. (a) Alkorta I, Rozas I, Elguero J. *J. Org. Chem.* 1997; **62**: 4687–4691; (b) Breinlinger EC, Keenan CJ, Rotello VM. *J. Am. Chem. Soc.* 1998; **120**: 8606–8609; (c) Gallivan JP, Dougherty DA. *Org. Lett.* 1999; **1**: 103–105.
12. (a) Umezawa Y, Nishio M. *Bioorg. Med. Chem.* 2000; **8**: 2643–2650; (b) Suezawa H, Yoshida T, Hirota M, Takahashi H, Umezawa Y, Honda K, Tsuboyama S, Nishio M. *J. Chem. Soc., Perkin Trans. 2* 2001; 2053–2058; (c) Ribas J, Cubero E, Luque FJ, Orozco M. *J. Org. Chem.* 2002; **67**: 7057–7065.
13. (a) Wulff G, Schmidt H, Witt H, Zentel R. *Angew. Chem., Int. Ed. Engl.* 1994; **33**: 188–191; (b) Robertson A, Shinkai S. *Coord. Chem. Rev.* 2000; **205**: 157–199; (c) Fiammengo R, Crego-Calama M, Reinhoudt DN. *Curr. Opin. Chem. Biol.* 2001; **5**: 660–673; (d) Satz AL, Bruice TC. *Bioorg. Med. Chem.* 2002; **10**: 241–252; (e) Ajayaghosh A, George SJ. *J. Am. Chem. Soc.* 2001; **123**: 5148–5149.
14. (a) Glusker JP. *Top. Curr. Chem.* 1998; **198**: 1–56; (b) Martin CB, Mulla HR, Willis PG, Cammers-Goodwin A. *J. Org. Chem.* 1999; **64**: 7802–7806; (c) Tsuzuki S, Honda K, Uchimaru T, Mikami M, Tanabe K. *J. Am. Chem. Soc.* 2002; **124**: 104–112.
15. (a) Kim E, Paliwal S, Wilcox CS. *J. Am. Chem. Soc.* 1998; **120**: 11192–11193; (b) de Frutos O, Gómez-Lor B, Granier T, Monge MA, Gutiérrez-Puebla E, Echavarren AM. *Angew. Chem., Int. Ed. Engl.* 1999; **38**: 204–207; (c) Zhang W, Horoszewski D, Decatur J, Nuckolis C. *J. Am. Chem. Soc.* 2003; **125**: 4870–4873; (d) Tsou LK, Tatko CD, Waters ML. *J. Am. Chem. Soc.* 2002; **124**: 14917–14921; (e) Aravinda S, Shamala N, Das C, Sriranjini A, Karle IL, Balaram P. *J. Am. Chem. Soc.* 2003; **125**: 5308–5315.
16. (a) Desiraju GR, Sharma CVKM. *J. Chem. Soc., Chem. Commun.* 1991; 1239–1240; (b) Coates GW, Dunn AR, Henling LM, Ziller JW, Lobkovsky EB, Grubbs RH. *J. Am. Chem. Soc.* 1998; **120**: 3641–3649; (c) Kim JH, Lindeman SV, Kochi JK. *J. Am. Chem. Soc.* 2001; **123**: 4951–4959; (d) Martin C, Mailliet P, Maddaluno J. *J. Org. Chem.* 2001; **66**: 3797–3805; (e) Matsumoto A, Tanaka T, Tsubouchi T, Tashiro K, Saragai S, Nakamoto S. *J. Am. Chem. Soc.* 2002; **124**: 8891–8902.
17. (a) Hunter CA. *Chem. Soc. Rev.* 1994; 101–109; (b) Engelkamp H, Middelbeek S, Nolte RJM. *Science* 1999; **284**: 785–788; (c) Frontera A, Garau C, Quiñonero D, Ballester P, Costa A, Deyá PM. *Org. Lett.* 2003; **5**: 1135–1138.
18. (a) Desiraju GR, Steiner T. *The Weak Hydrogen Bond in Structural Chemistry and Biology*. Oxford University Press: Oxford, 1999; (b) Zauhaur RJ, Colbert CL, Morgan RS, Welsh WJ. *Biopolymers* 2000; **53**: 233–248; (c) Steiner T, Koellner G. *J. Mol. Biol.* 2001; **305**: 535–557; (d) Clyburne JAC, Hamilton T, Jenkins HA. *Cryst. Eng.* 2001; **4**: 1–9; (e) Choudhury AR, Urs UK, Guru Row TN, Nagarajan K. *J. Mol. Struct.* 2002; **605**: 71–77; (f) Paul PKC. *Cryst. Eng.* 2002; **5**: 3–8.
19. (a) Wan QH, Ramaley L, Guy R. *Anal. Chem.* 1997; **69**: 4581–4585; (b) Nishimura J, Nakamura Y, Hayashida Y, Kudo T. *Acc. Chem. Res.* 2000; **33**: 679–686.
20. (a) Martínez A, Fernández E, Castro A, Conde S, Rodríguez-Franco I, Baños JE, Badía A. *Eur. J. Med. Chem.* 2000; **35**: 913–922; (b) Boger DL, Goldberg J, Silletti S, Kessler T, Cheresh DA. *J. Am. Chem. Soc.* 2001; **123**: 1280–1288; (c) Box VGS, Jean-Mary F. *J. Mol. Mod.* 2001; **7**: 334–342; (d) Manderson GA, Johansson JS. *Biochemistry* 2002; **41**: 4080–4087.
21. (a) Soriano MR, Lado-Touriño I, Tsobnang F. *Bull. Soc. Chim. Fr.* 1997; **134**: 1075–1081 (b) Dai C, Nguyen P, Marder TB, Scott AJ, Clegg W, Viney C. *Chem. Commun.* 1999; 2493–2494; (c) Gin DL, Gray DH, Smith RC. *Synlett* 1999; 1509–1522; (d) Menger FM, Caran KL. *J. Am. Chem. Soc.* 2000; **122**: 11679–11691; (e) Moore AJ, Chesney A, Bryce MR, Batsanov AS, Kelly JF, Howard JAK, Perepichka IF, Perepichka DF, Meshulam G, Berkovic G, Kotler Z, Mazor R, Khodorkovsky V. *Eur. J. Org. Chem.* 2001; 2671–2678; (f) Ajayaghosh A, George SJ. *J. Am. Chem. Soc.* 2001; **123**: 5148–5149; (g) Percec V, Glodde M, Bera TK, Miura Y, Siyanovskaya I, Singer KD, Balagurusamy VSK, Helney PA, Schnell I, Rapp A, Splass HW, Hudson SD, Duan H. *Nature (London)* 2002; **419**: 384–387.
22. (a) Heaton NJ, Bello P, Herradón B, del Campo A, Jiménez-Barbero J. *J. Am. Chem. Soc.* 1998; **120**: 9632–9645; (b) Bello P. PhD Thesis, University Complutense, Madrid, 1998.
23. (a) Bello P, Chana A, Heaton NJ, Maestro MA, Mahía J, Herradón B. *J. Mol. Struct.* 2001; **569**: 71–80; (b) Mann E, Mahía J, Maestro MA, Herradón B. *J. Mol. Struct.* 2002; **641**: 101–107; (c) Mann E, Montero A, Maestro MA, Herradón B. *Helv. Chim. Acta* 2002; **85**: 3624–3638.
24. (a) Chana A, Concejero MA, de Frutos M, González MJ, Herradón B. *Chem. Res. Toxicol.* 2002; **15**: 1514–1526; (b) Navas JM, Chana A, Herradón B, Segner H. *Environ. Toxicol. Chem.* 2003; **22**: 830–836.
25. (a) Newcombe LF, Gellman SH. *J. Am. Chem. Soc.* 1994; **116**: 4993–4994; (b) Newcomb LF, Haque TS, Gellman SH. *J. Am. Chem. Soc.* 1995; **117**: 6509–6519; (c) Hwang HJ, Lee SK, Lee S, Park JW. *J. Chem. Soc., Perkin Trans. 2* 1999; 1081–1086; (d) McKay SL, Haptonstall B., Gellman SH. *J. Am. Chem. Soc.* 2001; **123**: 1244–1245; (e) Sánchez M, Maestre I, Jaime C, Virgili A. *Tetrahedron: Asymmetry* 2001; **12**: 1737–1740; (f) Zych AJ, Iverson BL. *Helv. Chim. Acta* 2002; **85**: 3294–3300.
26. (a) Guckian KM, Schweitzer BA, Ren RXF, Sheils CJ, Tahmassebi DC, Kool ET. *J. Am. Chem. Soc.* 2000; **122**: 2213–2222; (b) Rashkin MJ, Waters ML. *J. Am. Chem. Soc.* 2002; **124**: 1860–1861.
27. (a) Heaton NJ, Bello P, Bello A, Riande E. *Macromolecules* 1997; **30**: 7536–7545; (b) Bello P, Bello A, Riande E, Heaton NJ. *Macromolecules* 2001; **34**: 181–186.
28. (a) Voigt-Martin IG, Durst H, Brzeezinski V, Krug H, Kreuder W, Ringsdorf H. *Angew. Chem., Int. Ed. Engl.* 1989; **28**: 323–325; (b) Collings PJ. *Liquid Crystals. Nature's Delicate Phase of Matter*. Adam Hilger: Bristol, 1990; (c) Tschierske C. *J. Mater. Chem.* 1998; **8**: 1485–1508.
29. (a) Williams JH, Cockcroft JK, Fitch AN. *Angew. Chem., Int. Ed. Engl.* 1992; **31**: 1655–1657; (b) Williams JH. *Acc. Chem. Res.* 1993; **26**: 593–598; (c) Cozzi F, Cinquini M, Annunziata R, Siegel JS. *J. Am. Chem. Soc.* 1993; **115**: 5330–5331; (d) Kim E, Paliwal S, Wilcox CS. *J. Am. Chem. Soc.* 1998; **120**: 11192–11193.
30. (a) Ligabue A, Soncini A, Lazzeretti P. *J. Am. Chem. Soc.* 2002; **124**: 2008–2014; (b) Lazzeretti P. *Prog. Nucl. Mag. Reson.* 2000; **36**: 1–88.
31. Flory PJ. *Macromolecules* 1974; **7**: 381–392.
32. Bovey FA. *Nuclear Magnetic Resonance Spectroscopy*. Academic Press: San Diego, 1988.
33. Stott K, Stonehouse J, Keeler J, Hwang TL, Shaka AJ., *J. Am. Chem. Soc* 1995; **117**: 4199–4200.
34. Macura S, Ernst RR. *Mol. Phys.* 1980; **41**: 95–117.
35. Allinger NL, Yuh YH, Lii JH. *J. Am. Chem. Soc.* 1989; **111**: 8551–8566.
36. Young DC. *Computational Chemistry: A Practical Guide for Applying Technique to Real-world Problems*. Wiley: New York, 2001.
37. Cramer CJ. *Essentials of Computational Chemistry. Theory and Models*. John Wiley: New York, 2002.

38. Case DA, Pearlman DA, Caldwell JW, Chetham TE III, Wang J, Ross WS, Simmerling CL, Darden TA, Merz KM, Stanton RV, Cheng AL, Vincent JJ, Crowley M, Tsui V, Gohlke H, Radmer RJ, Duan Y, Pitera J, Massova I, Seibel GL, Singh UC, Weiner PK, Kollman PA. *AMBER 7*. University of California: San Francisco, 2002.
39. (a) Lee C, Yang W, Parr RW. *Phys. Rev. B* 1998; **37**: 785–789; (b) Becke AD. *Phys. Rev. A* 1998; **38**: 3098–3100; (c) Becke AD. *J. Chem. Phys.* 1993; **98**: 1372–1377; (d) Parr, RG, Yang, W. *Density-functional Theory of Atoms and Molecules*. Oxford University Press: New York, 1989; (e) Koch W, Holthausen MC. *A Chemist's Guide to Density Functional Theory* (2nd edn). Wiley-VCH: Weinheim, 2001.
40. Frisch MJ, Trucks GW, Schlegel HB, Scuseria GE, Robb MA, Cheeseman JR, Zakrzewski VG, Montgomery JA Jr, Stratmann RE, Burant JC, Dapprich S, Millam JM, Daniels AD, Kudin KN, Strain MC, Farkas O, Tomasi J, Barone V, Cossi M, Cammi R, Mennucci B, Pomelli C, Adamo C, Clifford S, Ochterski J, Petersson GA, Ayala PY, Cui Q, Morokuma K, Salvador P, Dannenberg JJ, Malick DK, Rabuck AD, Raghavachari K, Foresman JB, Cioslowski J, Ortiz JV, Baboul AG, Stefanov BB, Liu G, Liashenko A, Piskorz P, Komaromi I, Gomperts R, Martin RL, Fox DJ, Keith T, Al-Laham MA, Peng CY, Nanayakkara A, Challacombe M, Gill PMW, Johnson B, Chen W, Wong MW, Andres JL, Gonzalez C, Head-Gordon M, Replogle S, and Pople, JA. *Gaussian 98, Revision A3*. Gaussian: Pittsburgh, PA, 1998.
41. Riande E, Saiz E. *Dipole Moments and Birefringence of Polymers.* Prentice-Hall: Englewood Cliffs, NJ, 1992.
42. Chablo A, Cruickshank DWJ, Hinchliffe A, Munn RW. *Chem. Phys. Lett.* 1981; **78**: 424–428.

